ChemComm

Cite this: *Chem. Commun.*, 2012, **48**, 10529–10531

www.rsc.org/chemcomm

COMMUNICATION

# A near-infrared fluorescent turn-on probe for fluorescence imaging of hydrogen sulfide in living cells based on thiolysis of dinitrophenyl ether†

**Xiaowei Cao, Weiying Lin,* Kaibo Zheng and Longwei He**

*Received 6th June 2012, Accepted 6th September 2012*
**DOI: 10.1039/c2cc34031c**



**We have constructed a novel NIR fluorescent turn-on hydrogen sulfide probe suitable for fluorescent imaging in living cells based on thiolysis of dinitrophenyl ether.**

Hydrogen sulfide ($H_2S$), traditionally considered to be a toxic gas with the typical smell of rotten eggs, has emerged as a member of the endogenous gaseous transmitter family of signaling molecules including nitric oxide (NO) and carbon monoxide (CO).[1–3] The endogenous production of $H_2S$ from a cysteine substrate or its derivatives is catalysed by several enzymes such as cystathionine β-synthase, cystathionine γ-lyase, and 3-mercaptopyruvate sulphurtransferase[4–6] in distinct mammalian tissues. $H_2S$ is endogenously produced in mitochondria and/or cytosol depending on the species and organs.[7] $H_2S$ may interact with downstream proteins by post-translational cysteine sulfhydration[8] and binding to heme iron centers,[9] which regulates various physiological processes including ischemia reperfusion injury,[10] vasodilation,[11] apoptosis,[12] angiogenesis,[13] neuromodulation,[14] inflammation,[15] insulin signaling,[16] and oxygen sensing.[17] Furthermore, $H_2S$ also serves as an antioxidant or scavenger for reactive oxygen species (ROS).[18] However, abnormal levels of $H_2S$ are associated with various diseases, like Alzheimer's disease[19] and Down syndrome.[20]

Detection of $H_2S$ in living systems has attracted great attention recently. The current techniques for $H_2S$ detection include colorimetric[21] and electrochemical[22] methods, chromatography,[23] and sulfide precipitation.[24] However, these methods require the living bio-samples to be post-mortem processed and destructed. Thus, these methods are destructive and not suitable for monitoring $H_2S$ in the native biological environment.

By contrast, fluorescence imaging provides an attractive technique to study biomolecules in live cells. Recently, a limited number of well-designed turn-on type fluorescent probes for $H_2S$ have been constructed. For instance, He's group developed selective fluorescent $H_2S$ probes on the basis of $H_2S$-induced tandem chemical reactions.[25] The $H_2S$-mediated reduction of azides to fluorescent amines has been employed to construct fluorescent $H_2S$ probes by Chang's,[26] Wang's,[27] and Han's[28] groups. Xian *et al.* introduced a turn-on strategy for fluorescent $H_2S$ probes based on a $H_2S$-triggered benzothiolone compounds formation.[29] Nagano's group reported a fluorescent probe for $H_2S$ by utilizing azamacrocyclic copper(II) ion complex chemistry to regulate the fluorescence.[30] Pluth's group constructed fluorescence turn-on probes for $H_2S$ *via* $H_2S$-mediated reduction of the nitro group to amines.[31]

Herein, we present the development of **NIR-$H_2S$** (Scheme 1), a unique type of a fluorescent turn-on probe for $H_2S$ based on dinitrophenyl ether chemistry. The dinitrophenyl group is often used for the protection of tyrosine in peptide synthesis. The removal of the dinitrophenyl protective group is conducted using thiols as the thiolyting agents under basic conditions.[32] $H_2S$ is a small gas molecule and has a p$K_a$ of around 6.9,[33] while the typical cellular free thiols (*i.e.* glutathione, cysteine) have higher p$K_a$ values about 8.5.[34] Thus, based on the marked distinctions in terms of size and p$K_a$ values, we envisioned that, at physiological pH, the thiolysis of the dinitrophenyl ether reaction may be chemoselective for $H_2S$ over biologically abundant glutathione and cysteine.

Compound **NIR-$H_2S$** was readily synthesized in two steps (Scheme 1). Condensation of the BODIPY **1** with Fisher aldehyde **2** afforded the intermediate **3**, which was then treated with 1-fluoro-2,4-dinitrobenzene under the basic conditions to give the target compound **NIR-$H_2S$** by a nucleophilic substitution. The structures of the compounds synthesized were fully characterized by the standard NMR and mass spectrometry.

We first evaluated the capability of **NIR-$H_2S$** to detect $H_2S$ in aqueous buffer. The titration of NaHS (a standard source

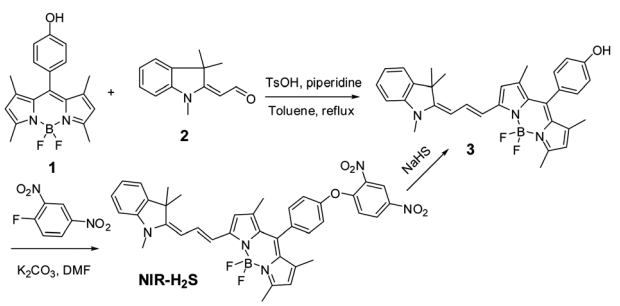


**Scheme 1** Design and synthesis of the NIR fluorescent turn-on probe **NIR-$H_2S$**.

*State Key Laboratory of Chemo/Biosensing and Chemometrics, College of Chemistry and Chemical Engineering, Hunan University, Changsha, Hunan 410082, P. R. China.*
*E-mail: weiyinglin@hnu.edu.cn; Fax: +86-731-88821464*
† Electronic supplementary information (ESI) available: Experimental procedures, characterization data, and additional spectra. See DOI: 10.1039/c2cc34031c

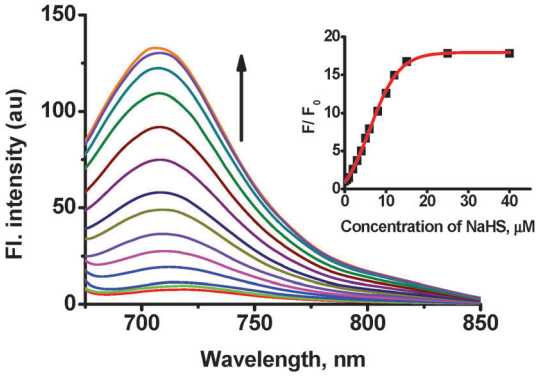


**Fig. 1** Fluorescence spectra of the probe **NIR-$H_2S$** (5.0 μM) in the aqueous buffer in the presence of different concentrations of NaHS (0–40 μM). Inset: fluorescence intensity ratio ($F/F_0$) changes at 708 nm of the probe **NIR-$H_2S$** (5.0 μM) with the amount of NaHS. Excitation at 650 nm. Emission at 708 nm.

for hydrogen sulfide) to the probe **NIR-$H_2S$** was performed in 50 mM PBS buffer (pH 7.0) with 3 mM cetyltrimethylammonium bromide (CTAB) and 10% ethanol. The free probe was essentially non-fluorescent in the buffer (Fig. 1). However, introduction of NaHS elicited a significant fluorescence turn-on response (18-fold fluorescence enhancement) at 708 nm (inset of Fig. 1). Notably, the emission wavelength of the probe is in the near-infrared (NIR) region, which is favorable for fluorescent imaging studies.[35] Furthermore, the fluorescence intensities at 708 nm have an excellent linear relationship with the concentrations of NaHS (Fig. S1, ESI†). **NIR-$H_2S$** responded rapidly to NaHS (Fig. S2, ESI†), and the pseudo-first-order rate constant was calculated to be $k = 0.006\ s^{-1}$ (Fig. S3, ESI†). The pH effect studies suggest that the maximal fluorescent signal was observed at around physiological pH (Fig. S4, ESI†). The detection limit was calculated to be $5 \times 10^{-8}$ M (S/N = 3), indicating that the probe is highly sensitive and may be suitable for studies of $H_2S$ in the living systems.

To shed light on the $H_2S$-triggered fluorescence turn-on response, we decided to characterize the thiolysis product and carry out theoretical calculations. The ESI-MS titration suggests the formation of compound **3** upon incubation of **NIR-$H_2S$** with NaHS (Fig. S5, ESI†), The thiolysis product **3** was further isolated and characterized by $^1H$ NMR, $^{13}C$ NMR, MS (EI), and HRMS (EI) (see the Experimental section, Fig. S6, ESI†). Furthermore, dinitrobenzene and the thiolysis product **3** (the NIR dye) were examined by density function theory (DFT) and time-dependent density function theory (TD-DFT) calculations in the B3LYP/6-31G(d) level of Gaussian 09 program. The large oscillator strength (0.8823) of the $S_0$ to $S_1$ transition suggests that the $S_1$ state in compound **3** is emissive (Table S1, ESI†). In addition, the LUMO of the dye **3** is significantly higher than that of dinitrobenzene, suggesting that the photo-induced electron transfer (PET) process from the excited dye **3** to the dinitrobenzene moiety is thermodynamically favorable (Fig. S7, ESI†). Thus, **NIR-$H_2S$** is essentially nonfluorescent likely due to efficient PET. However, after the dinitrobenzene moiety is removed by $H_2S$, nonfluorescent **NIR-$H_2S$** is converted into fluorescent **3** to elicit a $H_2S$-triggered fluorescence turn-on signal. Notably, treatment of NaHS to the probe induced no marked changes in the maximal absorption wavelength (Fig. S8, ESI†), further substantiating the PET signaling mechanism.

To examine the selectivity, the probe **NIR-$H_2S$** (5 μM) was treated with various biologically relevant species (*e.g.*, the representative anions, metal ions, reactive oxygen species, reactive nitrogen species, reducing agents, small-molecule thiols, and NaHS) in the aqueous buffer. As shown in Fig. 2, addition of the representative anions ($Cl^-$, $Br^-$, $I^-$, $AcO^-$, $N_3^-$, $CN^-$, $CO_3^{2-}$, $NO_2^-$) at 1 mM, metal ions ($K^+$, $Mg^{2+}$, $Ca^{2+}$, $Zn^{2+}$) at 1 mM, reactive oxygen and nitrogen species ($H_2O_2$, $OCl^-$, $^{\bullet}OH$, $^1O_2$, NO), and reducing agents (ascorbic acid, $S_2O_3^{2-}$, $SO_3^{2-}$) at the biologically relevant concentrations induced no marked fluorescence enhancement. Notably, small-molecule thiols such as glutathione (GSH) at 10 mM and cysteine at 1 mM triggered only a small fluorescence enhancement (3-fold) and have nearly no interference to $H_2S$ detection (Fig. S9, ESI†). By contrast, upon treatment of NaHS (25 μM) with the probe, a large fluorescence signal (18-fold fluorescence enhancement) was observed. Thus, these data demonstrate that the probe **NIR-$H_2S$** has a high selectivity for $H_2S$ over other biological species tested including glutathione (GSH) and cysteine at the biologically relevant concentrations, validating the hypothesis that the $H_2S$-triggered thiolysis of the dinitrophenyl ether reaction is chemoselective for $H_2S$ over other free thiols in the biological systems. The selectivity of the probe **NIR-$H_2S$** is superior or comparable to the known fluorescent $H_2S$ probes.

Due to the different environments between in solution and in live cells, we decided to further investigate the suitability of the probe to visualize $H_2S$ in living cells. First, the MTT assays for the probe **NIR-$H_2S$** and the released nitro product were conducted, and the results showed that both compounds with a concentration at 5 μM have only minimal cytotoxicity after a long period (24 h) (Fig. S10, ESI†). Thus, the probe at 5 μM was selected for imaging experiments in living cells.

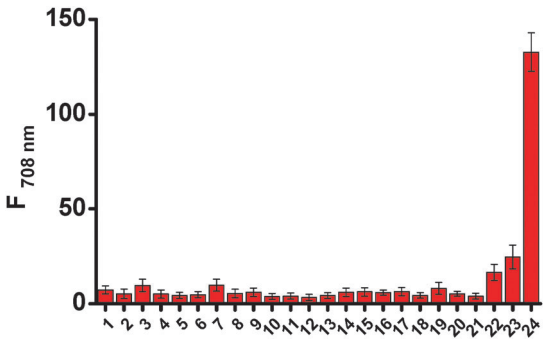


**Fig. 2** Fluorescence responses of the probe **NIR-$H_2S$** (5.0 μM) to various biologically relevant species in the aqueous buffer. Red bars represent the addition of an excess of the representative anions, metal ions, reactive oxygen species, reactive nitrogen species, reducing agents, small-molecule thiols, and NaHS (1 mM for $Cl^-$, $Br^-$, $I^-$; $CH_3COO^-$, $NO_2^-$, $N_3^-$,$CO_3^{2-}$, $K^+$, $Ca^{2+}$, $Mg^{2+}$ and $Zn^{2+}$, 50 μM for $CN^-$, $ClO^-$, $^{\bullet}OH$, $^1O_2$, and NO, 100 μM for $H_2O_2$, $SO_3^{2-}$, and $S_2O_3^{2-}$, 1 mM for ascorbic acid and cysteine, 10 mM for GSH, and 25 μM for NaHS). 1, probe **NIR-$H_2S$** alone; 2, $Cl^-$; 3, $Br^-$; 4, $I^-$; 5, $CH_3COO^-$; 6, $NO_2^-$; 7, $N_3^-$; 8, $CN^-$; 9, $CO_3^{2-}$; 10, $K^+$; 11, $Ca^{2+}$; 12, $Mg^{2+}$; 13, $Zn^{2+}$; 14, $H_2O_2$; 15, $ClO^-$; 16, $^{\bullet}OH$; 17, $^1O_2$; 18, NO; 19, ascorbic acid; 20, $SO_3^{2-}$; 21, $S_2O_3^{2-}$; 22, cysteine; 23, GSH; 24, NaHS. Excitation at 650 nm. Emission at 708 nm.

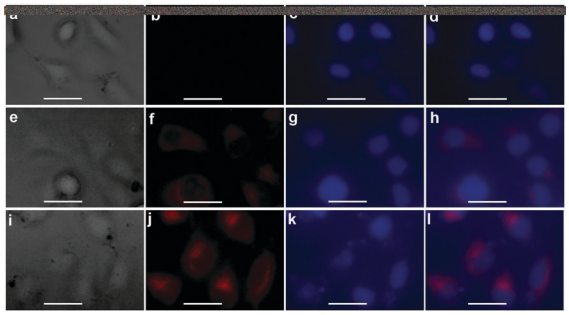

**Fig. 3** Fluorescence response of the probe **NIR-$H_2S$** with increasing concentrations of $H_2S$ in living MCF-7 cells. (a–l) The cells were pre-treated with the probe **NIR-$H_2S$** (5 μM) and Hoechst 33342 (5 μM) for 20 min, and then incubated with NaHS (b, c, d) 0 μM, (f, g, h) 10 μM, and (j, k, l) 100 μM for another 10 min. (a) Bright field image; (b) fluorescence image from the red channel; (c) fluorescence image from the blue channel (nuclear staining); (d) overlay of (b) with (c); (e) bright field image; (f) fluorescence image from the red channel; (g) fluorescence image from the blue channel (nuclear staining); (h) overlay of (f) with (g); (i) bright field image; (j) fluorescence image from the red channel; (k) fluorescence image from the blue channel (nuclear staining); (l) overlay of (j) with (k). Scale bar = 20 μm.

Toward this end, MCF-7 cells were pre-treated with the probe for 20 minutes, and then incubated with varying concentrations of NaHS for 10 minutes. As displayed in Fig. 3b, f and j, the fluorescence images in the red channel became brighter as the concentration of NaHS was increased from 0 to 100 μM. These data establish that the probe **NIR-$H_2S$** is cell membrane permeable and can report $H_2S$ in the living cells in a dose-dependent manner. It is worth noting that the nuclear staining with Hoechst 33 258 (Fig. 3c, d, g, h, k and l) implies that the cells were alive after treatment with the probe. In addition, mitochondria staining (Fig. S11c, e, h and j, ESI†) and nuclear staining (Fig. S11d, e, i and j, ESI†) reveal that the turn-on signal of the probe is mainly observed in the mitochondria of MCF-7 cells. Interestingly, this is in accordance with the report that $H_2S$ is primarily catabolized in mitochondria by thiosulfate reductase and sulfite oxidase.[7]

In summary, we have developed a unique NIR fluorescence turn-on $H_2S$ probe, **NIR-$H_2S$**, on the basis of dinitrophenyl ether chemistry, a new strategy for the design of fluorescent $H_2S$ probes. Furthermore, we have demonstrated that **NIR-$H_2S$** is suitable for fluorescent imaging in the living cells. The further utility of the design strategy and applications of this unique NIR fluorescent turn-on probe to investigate the biological functions and pathological roles of $H_2S$ is underway. In addition, we expect that the BODIPY–merocyanine conjugate (NIR dye **3**) will be useful as a NIR platform for the development of various NIR fluorescent probes.

This work was financially supported by NSFC (20972044, 21172063), NCET (08-0175), and the Doctoral Fund of Chinese Ministry of Education (20100161110008).

## Notes and references


1 R. Wang, *FASEB J.*, 2002, **16**, 1792.
2 E. Culotta and D. E. Koshland Jr, *Science*, 1992, **258**, 1862.
3 Y. Han, J. Qin, X. Chang, Z. Yang and J. Du, *Cell. Mol. Neurobiol.*, 2006, **26**, 101.
4 K. Tanizawa, *J. Biochem.*, 2011, **149**, 357.
5 D. Boehning and S. H. Snyder, *Annu. Rev. Neurosci.*, 2003, **26**, 105.
6 K. Abe and H. Kimura, *J. Neurosci.*, 1996, **16**, 1066.
7 P. Kamoun, *Amino Acids*, 2004, **26**, 243.
8 A. K. Mustafa, M. M. Gadalla, N. Sen, S. Kim, W. Mu, S. K. Gazi, R. K. Barrow, G. Yang, R. Wang and S. H. Snyder, *Sci. Signaling*, 2009, **2**, ra72.
9 E. Blackstone, M. Morrison and M. B. Roth, *Science*, 2005, **308**, 518.
10 J. W. Elrod, J. W. Calvert, J. Morrison, J. E. Doeller, D. W. Kraus, L. Tao, X. Jiao, R. Scalia, L. Kiss, C. Szabo, H. Kimura, C.-W. Chow and D. J. Lefer, *Proc. Natl. Acad. Sci. U. S. A.*, 2007, **104**, 15560.
11 G. Yang, L. Wu, B. Jiang, B. Yang, J. Qi, K. Cao, Q. Meng, A. K. Mustafa, W. Mu, S. Zhang, S. H. Snyder and R. Wang, *Science*, 2008, **322**, 587.
12 G. Yang, L. Wu and R. Wang, *FASEB J.*, 2006, **20**, 553.
13 A. Papapetropoulos, A. Pyriochou, Z. Altaany, G. Yang, A. Marazioti, Z. Zhou, M. G. Jeschke, L. K. Branski, D. N. Herndon, R. Wang and C. Szabó, *Proc. Natl. Acad. Sci. U. S. A.*, 2009, **106**, 21972.
14 K. Abe and H. Kimura, *J. Neurosci.*, 1996, **16**, 1066.
15 L. Li, M. Bhatia, Y. Z. Zhu, Y. C. Zhu, R. D. Ramnath, Z. J. Wang, F. B. Anuar, M. Whiteman, M. Salto-Tellez and P. K. Moore, *FASEB J.*, 2005, **19**, 1196.
16 W. Yang, G. D. Yang, X. M. Jia, L. Y. Wu and R. Wang, *J. Physiol.*, 2005, **569**, 519.
17 Y.-J. Peng, J. Nanduri, G. Raghuraman, D. Souvannakitti, M. M. Gadalla and G. K. Kumar, *Proc. Natl. Acad. Sci. U. S. A.*, 2010, **107**, 10719.
18 J. W. Calvert, S. Jha, S. Gundewar, W. J. Elrod, A. Ramachandran, C. B. Pattillo, C. G. Kevil and D. J. Lefer, *Circ. Res.*, 2009, **105**, 365.
19 K. Eto, T. Asada, K. Arima, T. Makifuchi and H. Kimura, *Biochem. Biophys. Res. Commun.*, 2002, **293**, 1485.
20 P. Kamoun, M.-C. Belardinelli, A. Chabli, K. Lallouchi and B. Chadefaux-Vekemans, *Am. J. Med. Genet.*, 2003, **116A**, 310.
21 X. Gu, C. Liu, Y.-C. Zhu and Y.-Z. Zhu, *Tetrahedron Lett.*, 2011, **52**, 5000.
22 (*a*) N. S. Lawrence, R. P. Deo and J. Wang, *Anal. Chim. Acta*, 2004, **517**, 131; (*b*) N. S. Lawrence, J. Davis, L. Jiang, T. G. J. Jones, S. N. Davies and R. G. Compton, *Electroanalysis*, 2000, **12**, 1453.
23 (*a*) J. Radford-Knaery and G. A. Cutter, *Anal. Chem.*, 1993, **65**, 976; (*b*) C. J. Richardson, E. A. M. Magee and J. H. Cummings, *Clin. Chim. Acta*, 2000, **293**, 115.
24 M. Ishigami, K. Hiraki, K. Umemura, Y. Ogasawara, K. Ishii and H. Kimura, *Antioxid. Redox Signaling*, 2009, **11**, 205.
25 Y. Qian, J. Karpus, O. Kabil, S.-Y. Zhang, H.-L. Zhu, R. Banerjee, J. Zhao and C. He, *Nat. Commun.*, 2011, **2**, 495.
26 A. R. Lippert, E. J. New and C. J. Chang, *J. Am. Chem. Soc.*, 2011, **133**, 10078.
27 H. Peng, Y. Cheng, C. Dai, A. L. King, L. B. Predmore, D. J. Lefer and B. Wang, *Angew. Chem., Int. Ed.*, 2011, **50**, 9672.
28 F. Yu, P. Li, P. Song, B. Wang, J. Zhao and K. Han, *Chem. Commun.*, 2012, **48**, 2852–2854.
29 (*a*) C. Liu, J. Pan, S. Li, Y. Zhao, L. Y. Wu, C. E. Berkman, A. R. Whorton and M. Xian, *Angew. Chem., Int. Ed.*, 2011, **50**, 10327; (*b*) C. Liu, B. Peng, S. Li, C.-M. Park, A. R. Whorton and M. Xian, *Org. Lett.*, 2012, **14**, 2184.
30 K. Sasakura, K. Hanaoka, N. Shibuya, Y. Mikami, Y. Kimura, T. Komatsu, T. Ueno, T. Terai, H. Kimura and T. Nagano, *J. Am. Chem. Soc.*, 2011, **133**, 18003.
31 L. A. Montoya and M. D. Pluth, *Chem. Commun.*, 2012, **48**, 4767.
32 (*a*) S. Shaltiel, *Biochem. Biophys. Res. Commun.*, 1967, **29**, 178; (*b*) R. Philosof-Oppenheimer, I. Pechtz and M. Fridkin, *Int. J. Pept. Protein Res.*, 1995, **45**, 116.
33 J. C. Mathai, A. Missner, P. Kügler, S. M. Saparov, M. L. Zeidel, J. K. Lee and P. Pohl, *Proc. Natl. Acad. Sci. U. S. A.*, 2009, **106**, 16633.
34 (*a*) M. P. Lutolf, N. Tirelli, S. Cerritelli, L. Cavalli and J. A. Hubbell, *Bioconjugate Chem.*, 2001, **12**, 1051; (*b*) C. N. Salinas and K. S. Anseth, *Macromolecules*, 2008, **41**, 6019.
35 *Near-Infrared Applications in Biotechnology*, ed. R. Raghavachari and M. Dekker, New York, 2001.